

# Optical analysis of light management for finger designs in CPV systems

Mengdi Liu  | Udo Römer  | Nicholas J. Ekins-Daukes  | Alison Lennon 

School of Photovoltaic and Renewable Energy Engineering, University of New South Wales, Sydney, Australia

## Correspondence

Mengdi Liu, School of Photovoltaic and Renewable Energy Engineering, University of New South Wales, Sydney 2052, Australia.  
Email: [mengdi.liu@unsw.edu.au](mailto:mengdi.liu@unsw.edu.au)

## Funding information

Australian Renewable Energy Agency, Grant/Award Number: 2017/RND002; Australian Research Council, Grant/Award Numbers: DE210100453, FT170100447

## Abstract

Concentrated photovoltaic (CPV) systems can achieve high energy conversion efficiencies due to their use of concentrating optics and highly efficient solar cells; however, power losses arising from the front surface reflection and metallization shading typically contribute a significant fraction to the total power loss for these devices. In flat silicon photovoltaic (PV) modules, the front-metal finger shape is often shaped to minimize shading losses. Finger shape is even more relevant for CPV cells where the current density and front metal shading are much higher. This study compares the optical performance of five light management finger designs in CPV systems with two different refractive homogenizers. The optical efficiency and loss analysis were determined using ray-tracing simulations. It is shown that shaped, light diverting metal fingers can improve the optical efficiency in CPV systems by up to 9.9% absolute compared to rectangular fingers, corresponding to an absolute cell efficiency increase of 3.0%. Although sharp edged triangular finger structures may be challenging to fabricate, significant optical gains can still be achieved with trapezoid or rounded cap finger shapes.

## KEYWORDS

concentrated photovoltaic, light management finger design, optical efficiency, secondary optical element

## 1 | INTRODUCTION

Solar energy technology is fast becoming an inexpensive and sustainable source of renewable electricity. Concentrated Photovoltaic (CPV) systems are well suited for MW scale solar power generation where both heat and electrical power are desirable. Sunlight can be collected using tracked mirrors or lenses and directed onto on a small receiver area covered by highly efficient photovoltaic solar cells with practical concentrations of up to 1,000 Suns being routinely achieved.<sup>1</sup> Fundamentally, operating a solar cell at high concentration increases the current of the device since the current increases in proportion to the solar concentration. The increased current also results in an increased  $V_{oc}$  which increases the cell efficiency.<sup>2</sup> However, delivering high

currents from the CPV solar cell is challenging since the front surface of the solar cell should remain as transparent as possible to sunlight yet also have sufficient metal coverage to pass these high currents (typically  $14 \text{ A cm}^{-2}$  at 1,000 Suns for dual-junction solar cells<sup>3</sup> and  $26 \text{ A cm}^{-2}$  for single junction solar cells<sup>4</sup>) with minimal resistive loss. A careful optimization of the front metal coverage is necessary and is usually performed at the cell level.

Optimization of metallization for CPV solar cells has focused on optimizing grid spacing, grid thickness, and metallization patterns under concentrated incidence.<sup>5–7</sup> Metal shapes, such as trapezoidal shapes, have been reported for CPV solar cells.<sup>8</sup> However, optimizing the metal grid shapes to enhance light capture under concentrated flux distribution has received little attention to date. For industrial

This is an open access article under the terms of the [Creative Commons Attribution-NonCommercial](https://creativecommons.org/licenses/by-nc/4.0/) License, which permits use, distribution and reproduction in any medium, provided the original work is properly cited and is not used for commercial purposes.

© 2022 The Authors. Progress in Photovoltaics: Research and Applications published by John Wiley & Sons Ltd.

flat-plate terrestrial silicon PV modules, surface structuring is routinely applied to interconnection ribbons (attached to cell busbars) to improve the optical performance of modules by either scattering the light incident on the ribbon to the module glass from where it is re-directed back into the cell or by re-directing incident light directly into the cell.<sup>9–14</sup> Metal finger shading can also be minimized by tuning the metal contact shape and/or surface. Kik<sup>15</sup> presented a grid structure with a surface tilt of 15° resulting in a transmittance of 86% with 50% metal coverage. Saive et al.<sup>16</sup> reported a micro-scale triangular cross-section finger structure, which can significantly reduce shading loss by redirecting incident light directly to the active cell area. These shaped contact structures are often loosely referred to as “transparent” contacts because reflection losses are reduced to small values (i.e., the contacts appear as if “transparent”). However, as demonstrated by Li et al.,<sup>14</sup> the performance of transparent contacts can deteriorate significantly if the incoming light is not directed at 90° to the surface of the solar cell. Although there is an opportunity to reduce effective metal shading in CPV systems using metal contact shaping, the resulting optical efficiency will depend on how the primary and secondary (if used) optical elements used in these systems impact the distribution of angles of the incident light on the solar cell surface.

Directly imaging the Sun onto the front surface of the solar cell results in a concentrated non-uniform flux distribution,<sup>17</sup> which can

lead to a non-uniform photon-generated current density and a consequent voltage drop arising from series resistance power losses in the emitter and contact/metal resistance losses of the solar cell.<sup>18,19</sup> Consequently, secondary optical elements, such as homogenizers, are employed to improve the homogeneity of the round focused flux that results from the primary concentrator.<sup>20</sup> However, although the solar flux can be effectively “homogenized” with this strategy, it is at the expense of the angular distribution of the incident light which increases during this process. Figure 1 schematically depicts PV systems under concentrated sunlight conditions with and without homogenizers and shows the flux distribution and angular distribution of corresponding CPV system on the solar cell surface. Unconcentrated sunlight irradiates parallel, but under concentration, the angular distribution expands with the concentration ratio. Figure 1B,C shows two different designs of homogenizer, one with straight sidewalls and a second with tapered sidewalls. Both designs can homogenize the light intensity across cell area as shown in Figure 1E,F. With straight sidewalls, the angular distribution extends to 19.2° owing to the increased refractive index of the homogenizer and with tapered sidewalls to 39.5° as shown in Figure 1H,I. This relatively large distribution of incident light angles needs to be considered when designing practical metal contact schemes. Indoor CPV cell test procedures vary the distance between the solar cell and illumination lamp in order to

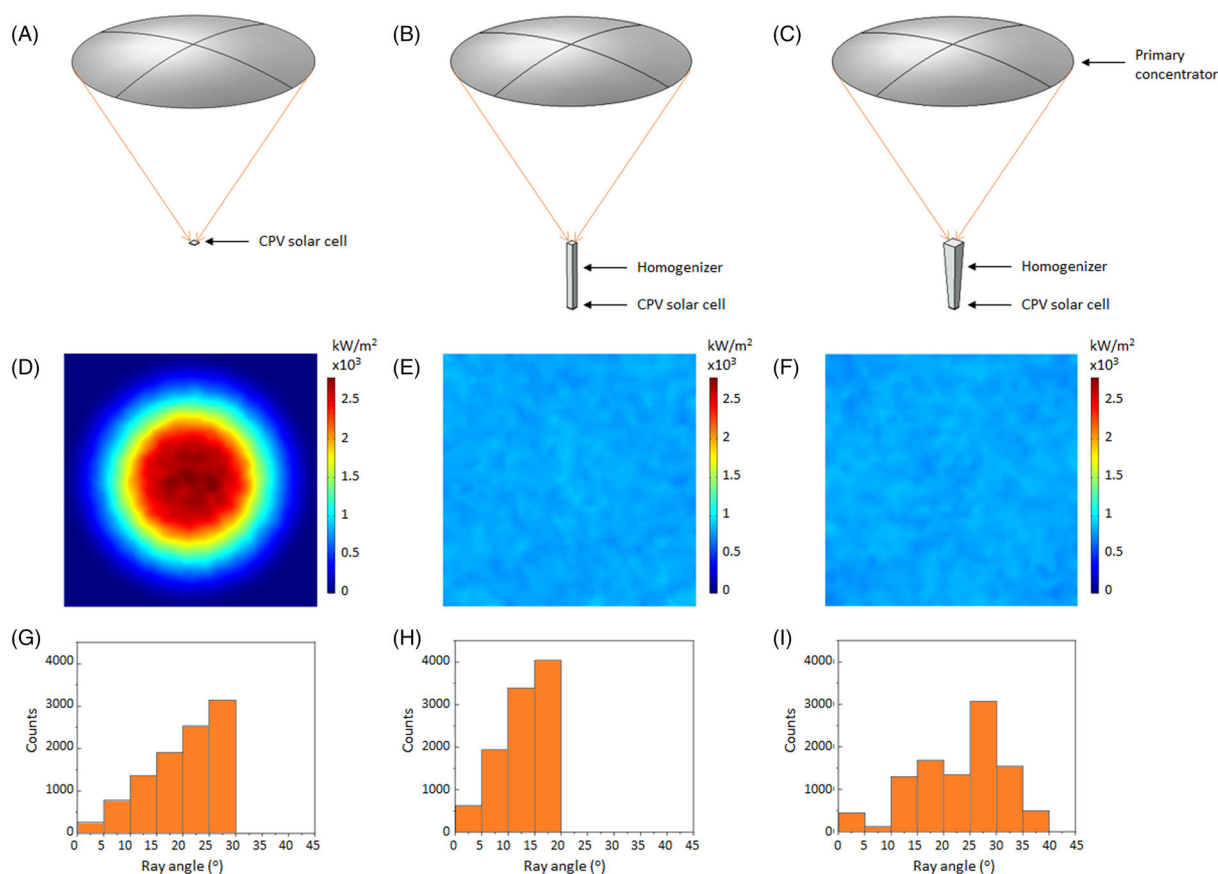


**FIGURE 1** Schematic showing three CPV systems: (A) a CPV system without a homogenizer; (B) a CPV system including a homogenizer with straight sidewalls; and (C) a CPV system including a homogenizer with tapered sidewalls. Flux distributions and angular distributions for corresponding CPV systems are shown in (D)–(F), and (g)–(I), respectively

change the concentration<sup>21</sup> and therefore do not account for the angular variation of photon flux with increasing cell concentration. The optimum metallization for a cell designed to achieve the highest efficiency under indoor testing will therefore not differ from one optimized for power generation in a practical CPV system.

In this study, the optical performance of five shaped finger designs was investigated in a CPV system comprising primary and secondary optical elements and a concentration of 1,200 Suns using ray-tracing simulations. Section 2 details the simulation methodology and the results of the simulations are evaluated and discussed in Section 3 using optical efficiency comparisons and ray loss analyses. It is concluded that the receiving cell efficiency can be increased by 10.5% relative by adopting a geometric finger structure that maximizes the light capture by the solar cell when operating within a CPV system comprising a parabolic dish primary concentrator and a homogenizer with straight/tapered sidewalls.

## 2 | SIMULATION METHODOLOGY

COMSOL Multiphysics® (Version 55) was used to simulate the optical transmittance using ray-tracing simulations. The CPV system modeled is shown schematically in Figure 2. It contains a primary concentrator, a homogenizer, and a CPV solar cell. The primary concentrator was assumed to be a paraboloidal dish with a geometric concentration ratio of 1,200 and a 30° rim angle. Solar radiation enters parallel from the top and is reflected by the primary concentrator. The rays converge towards a small area in the focal plane where the entrance to the homogenizer is placed. Refractive homogenizers of length 10 cm with straight and tapered sidewalls were compared in this study (see Figure 2B). The material assumed for both homogenizers was n-BK7 glass. The outlet shape of the homogenizer aligned with the shape of the underlying solar cell, which in this study was a square solar cell with an area of 1 cm<sup>2</sup>. The inlet shape for the homogenizer with tapered sidewalls was a square with a dimension of 2 cm, corresponding to a reduction in area at the homogenizer exit by a factor of 4. The CPV module was placed at the outlet of homogenizer. The material used for glass, encapsulant, and cell was n-BK7 glass,

Dow Corning PV-6100, and gallium arsenide (GaAs), respectively. The glass (above the cell) was assumed to be in intimate contact with the outlet of the homogenizer and therefore can be considered also as part of the homogenizer. A TiO<sub>2</sub>/SiO<sub>2</sub> dual anti-reflective coating (ARC) layer was assumed for the light-receiving surface of the solar cell. Five finger designs as shown in Figure 3 were investigated: rectangular finger (RF), trapezoid finger (TF), light scattering finger with V-groove cap (VCF), light scattering finger with round cap (RCF), and light diverting finger (LDF). All finger designs used the same finger spacing of 50 μm. This finger spacing was selected in order to reduce the power loss due to the lateral series resistance in the solar cell to be <1% at 500 Suns. The efficiency gain will depend strongly on finger spacing. With the exception of the LDF structure, unless otherwise stated, all finger structures had a constant cross-sectional area and constant bottom width of 5 μm, which leads to identical metal resistive losses and contact resistive losses. For the LDF structure, either the cross-sectional area or bottom width was maintained at a constant value. All finger surfaces were assumed to be perfect specular reflective surfaces.

Light rays were assumed to propagate through the homogenizer, glass, encapsulant, and ARC according to the real part of respective materials' refractive index. Absorption was not considered in this simulation. The reflected and refracted rays were traced through a boundary between media with different refractive indices based on Snell's law and the Fresnel equations implemented in COMSOL Multiphysics®. The wavelength used in all the simulations was 680 nm. The transmitted power was then collected by a detector plane which was placed under the ARC layer. The optical efficiency was calculated by comparing the input power to the CPV system with the power reached at the detected surface inside the solar cell. Losses from inlet (top loss) and sidewalls (side loss) of the homogenizer were also analyzed.

## 3 | RESULTS AND DISCUSSION

Figure 4 compares the optical efficiency and loss analysis for CPV cells with RFs and TFs for a homogenizer with straight sidewalls

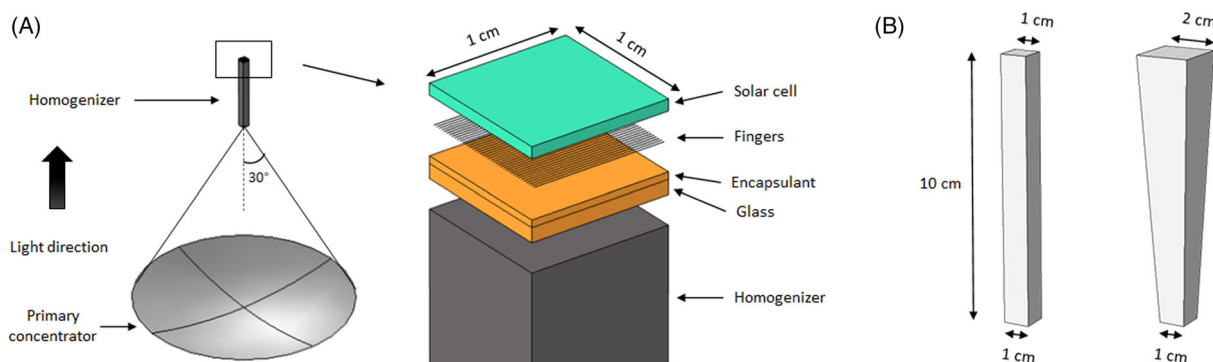


**FIGURE 2** (A) Schematic of the ray tracing model comprising a primary optic (parabolic dish) and a homogenizer and a solar cell receiver. (B) Dimensions of the two homogenizers evaluated in this study

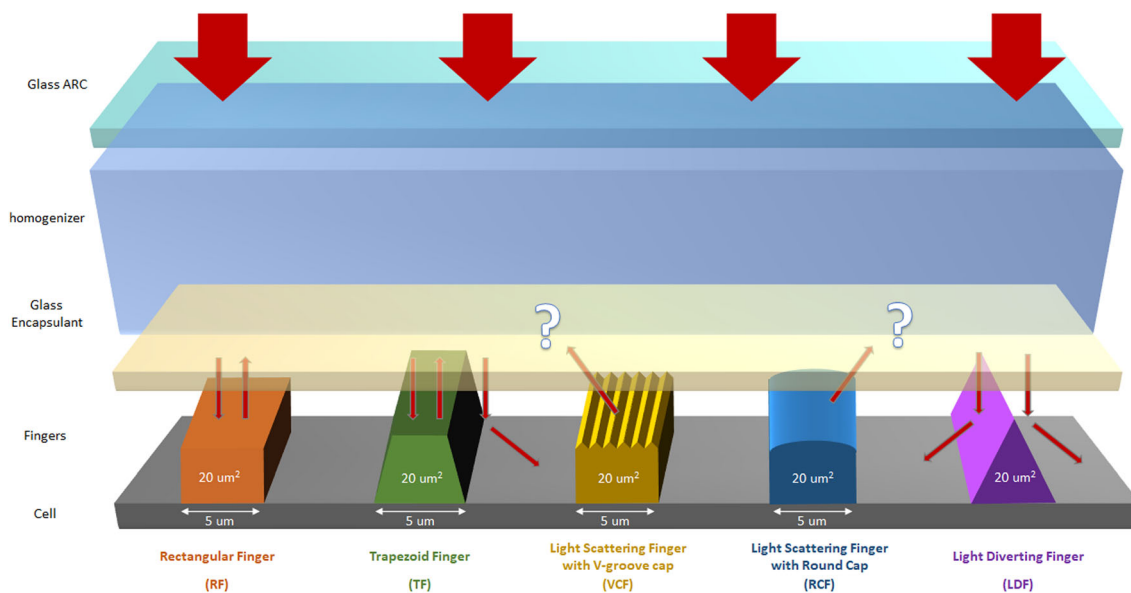


**FIGURE 3** Schematic showing the geometry of the five shaped finger designs evaluated. The question marks indicate light that is scattered at an angle towards the glass, the angle of scattering depending on the angle of the incident light, and the angle of the tilted or rounded surface of the finger

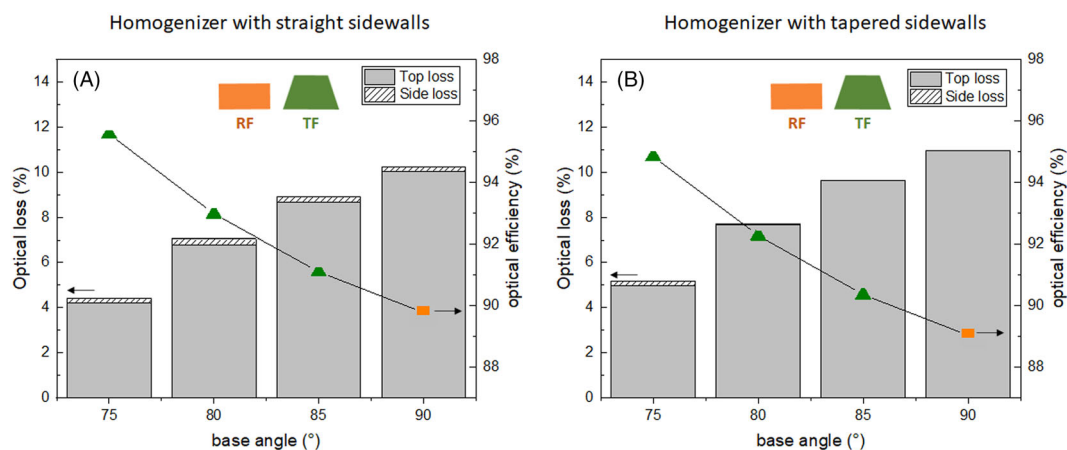
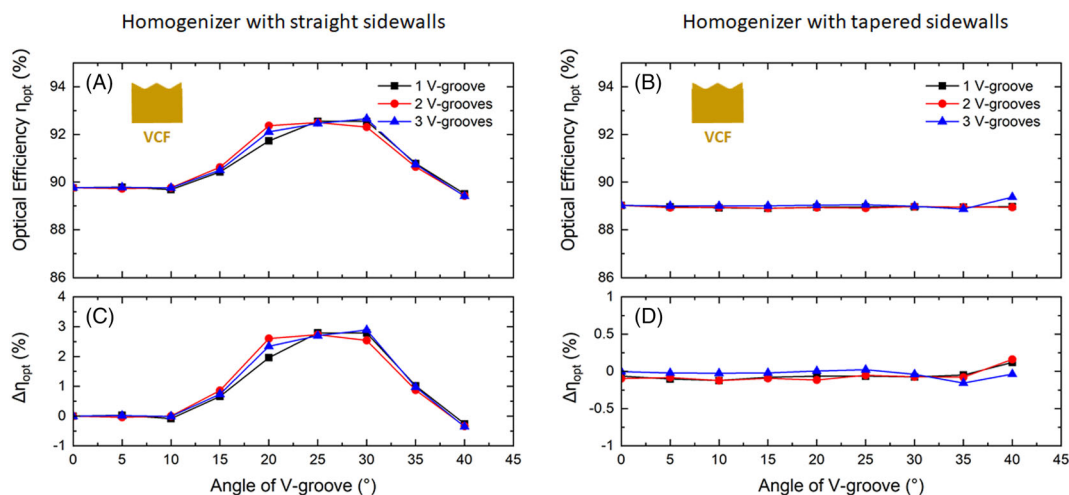


**FIGURE 4** Optical efficiency and loss for CPV cells with RF and TF structures with different base angles for a homogenizer with (A) straight and (B) tapered sidewalls. All fingers have a base width  $5 \mu\text{m}$  and finger cross-sectional area  $20 \mu\text{m}^2$

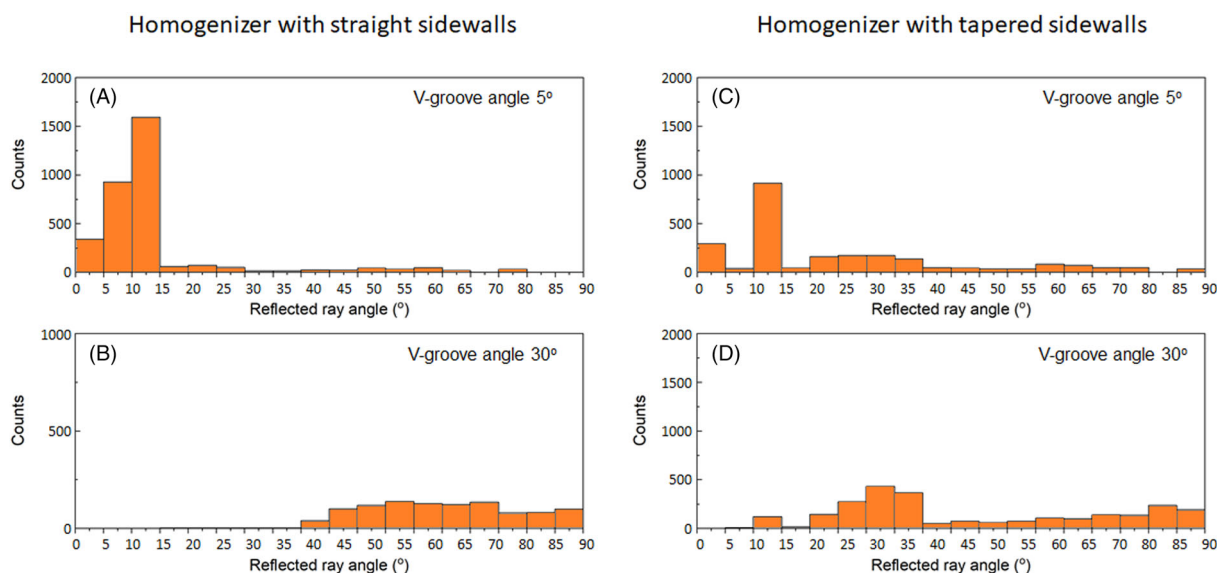
(Figure 4A) and tapered sidewalls (Figure 4B) for four different base angles of fingers ranging from  $75^\circ$  to  $90^\circ$ . The cross-sectional area and the finger base width were kept the same for all simulations for constant contact and finger line resistance. The TFs with a base angle of  $75^\circ$  result in the highest optical efficiency of 95.6% and 94.8% with the homogenizer with straight and tapered sidewalls, respectively. For both homogenizers, this represents a maximum increase of  $\sim 5.8\%$  in optical efficiency comparing to the RFs. The tapered finger sidewalls can redirect rays into the cell resulting in a larger optical efficiency. The constant cross-sectional area constraint also results in a reduced finger flat surface from where the light is reflected back into the homogenizer and ultimately lost.

Figure 5 compares the optical efficiency for CPV cells with VCF structure with different numbers of V-grooves. The V-groove angle

was correspondingly changed to ensure that the width and the cross-sectional area of the fingers were unchanged. The results show that VCF structures can improve the optical efficiency with a maximum increase of 2.7% at a V-groove angle of  $30^\circ$  in a CPV system with straight homogenizer sidewalls. However, for systems with tapered homogenizer sidewalls, the VCF structures offer no measurable benefit over the RF structure. For both homogenizers, it was found that the number of V-grooves does not affect the optical efficiency. Therefore, a two-V-groove cap structure was selected for further loss analysis. The reflected ray angle distribution and loss analysis for this VCF case are shown in Figures 6 and 7, respectively. For the CPV systems with straight homogenizer sidewalls, the angle of reflection is mostly within  $20^\circ$  at a V-groove angle of  $5^\circ$  but extends to almost  $90^\circ$  at a V-groove angle of  $30^\circ$ . The critical angle for total internal reflection



**FIGURE 5** Optical efficiency of CPV cells with VCF structures having different numbers of V-grooves for a homogenizer with (A) straight and (B) tapered sidewalls; (C) and (D) show the corresponding change in optical efficiency,  $\Delta\eta_{\text{opt}}$  (%)



**FIGURE 6** Reflected ray angle distributions for CPV cells with VCF structures with two V-grooves with angles of  $5^\circ$  (A and C) and  $30^\circ$  (B and D)

between glass/air interface is  $\sim 42^\circ$ . This means that ray angles less than the complementary angle of  $48^\circ$  will be totally reflected by the sidewalls of the homogenizer and reach the top surface of the homogenizer. At the top surface, light with ray angles less than  $42^\circ$  will partially propagate through the glass resulting in top losses, while rays with an angle between  $42^\circ$  and  $48^\circ$  will be total internally reflected back into the homogenizer. For the tapered homogenizer, the reflected ray angle range is predominantly within  $40^\circ$ . Since the tapered homogenizer has a shallow sidewall slope of  $2.9^\circ$ , rays with angles less than  $45.1^\circ$  will be total internally reflected by the side wall of homogenizer.

With practical fabrication methods, it can be difficult to form the sharp edges of V-grooves. Consequently, an optical efficiency comparison and loss analysis was performed for RCF structures with a

varied arc angle of the cap layer (see Figure 8). For both homogenizer types, the optical efficiency is proportional to the arc angle with a maximum increase of 3.10% and 2.43% for homogenizers with straight and tapered sidewalls, respectively. As observed for the VCF structures, with the RCF structures having a small arc angle, most rays can be reflected back with minor ray angle changes. Rays then travel through the homogenizer and are lost at the entrance of the homogenizer. Fingers with a large arc angle can increase the angular range of reflection, resulting in increased side losses which partially compensate the reduced losses at the top surface of the homogenizers.

Figure 9 compares the optical efficiency for CPV cells with LDF structures for varying finger base angles. Light diverting fingers with same bottom width or same cross-sectional area were considered, ensuring that either the contact resistance loss or the finger resistance

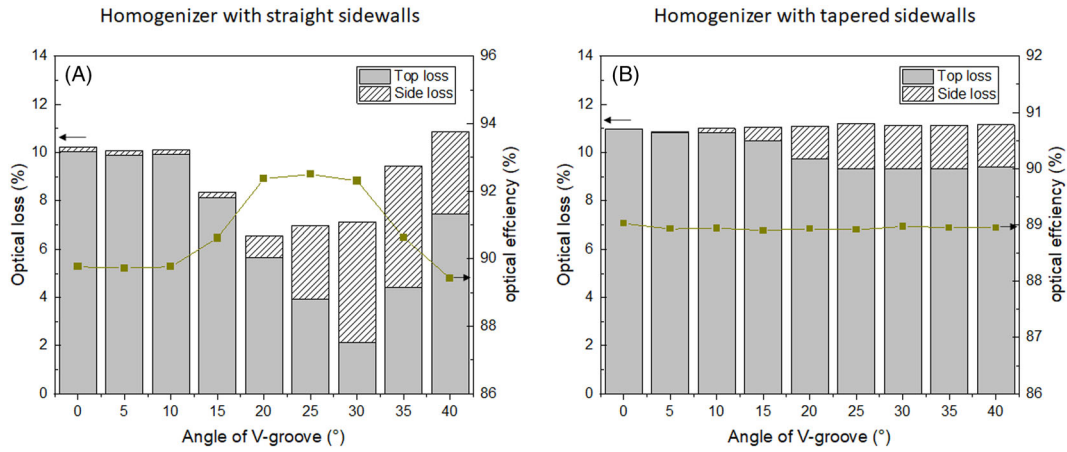


**FIGURE 7** Optical efficiency and loss for CPV cells with VCF structures with different V-groove angles for a homogenizer with (A) straight and (B) tapered sidewalls

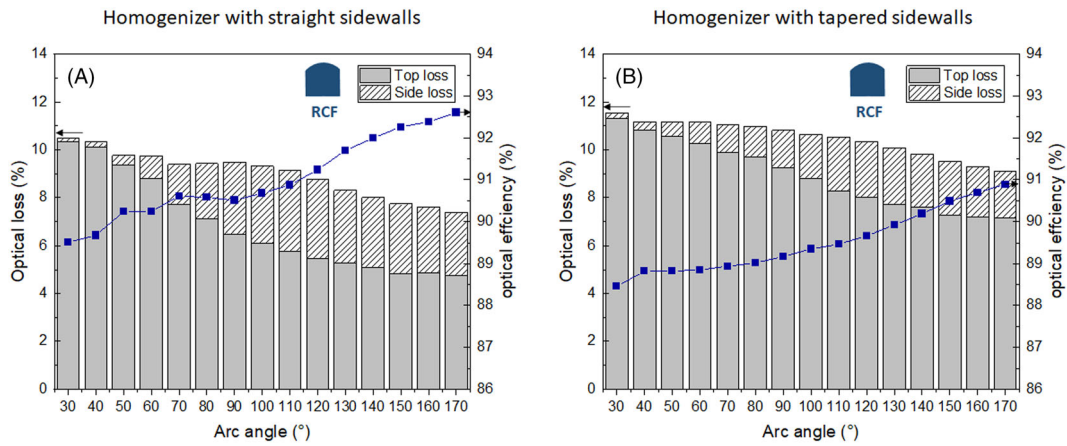


**FIGURE 8** Optical efficiency and loss for CPV cells with RCF structures with different rounded cap angles for a homogenizer with (A) straight and (B) tapered sidewalls

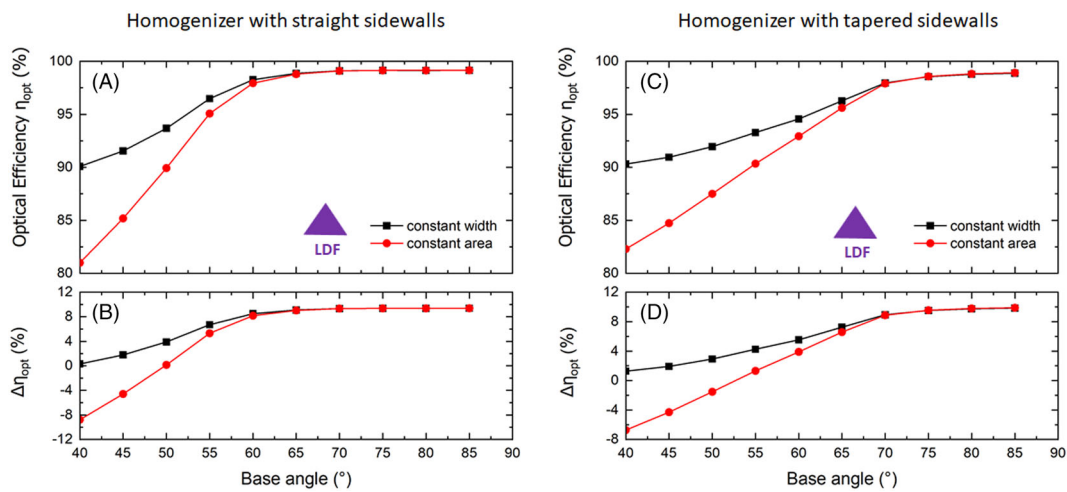


**FIGURE 9** Optical efficiency and loss for CPV cells with LDF structures with different base angles for a homogenizer with (A) straight and (C) tapered sidewalls; (B) and (D) show the corresponding changes in optical efficiency compared to a RF (width 5 μm; height 4 μm)

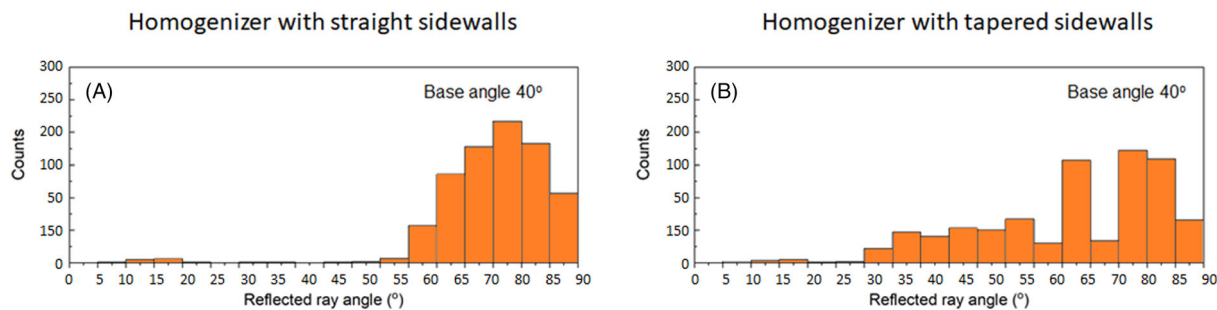


**FIGURE 10** Reflected ray angle distribution for CPV cells with LDF structures with constant area and a base angle of  $40^\circ$  for a homogenizer with (A) straight and (B) tapered sidewalls

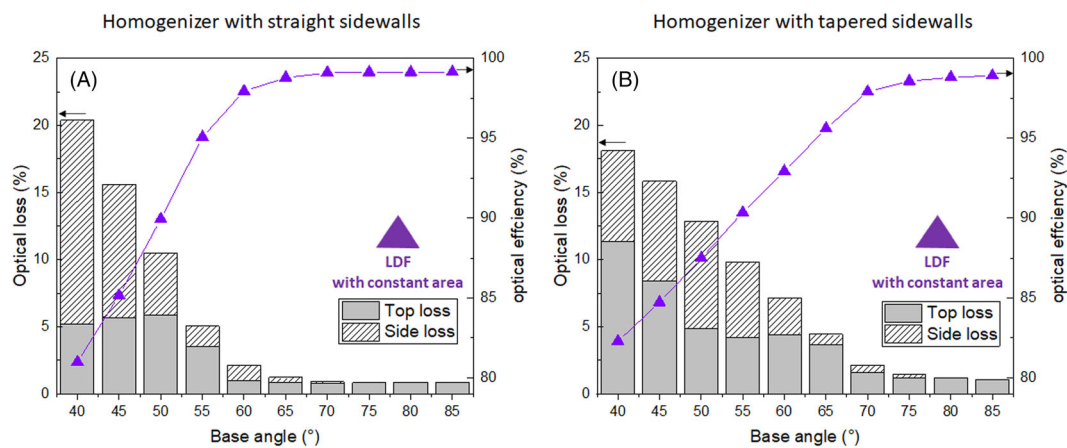


**FIGURE 11** Optical efficiency and loss for CPV cells with LDF structures with different base angles and constant finger area for a homogenizer with straight (A) and tapered (B) sidewalls

loss is kept constant. For both conditions, the optical efficiency increases with increasing finger base angle, reaching a maximum optical efficiency of 99.14% and 98.91% for CPV systems with straight and tapered homogenizer sidewalls, respectively. These are the highest optical efficiencies of all the investigated finger structures. Compared to RF structures with identical finger width or finger cross-sectional area, the optical efficiency increase is 9.37% and 9.88% for homogenizers with straight and tapered sidewalls, respectively.

An analysis of the reflected ray angle distribution and losses for LDFs with constant area are shown in Figures 10 and 11, respectively. Most rays reflected by fingers have an angle range between  $55^\circ$  and  $90^\circ$  leading to side losses for LDF with a base angle of  $40^\circ$ . When the base angle is larger than  $75^\circ$  in CPV systems with straight homogenizers, all rays incident on the fingers can be reflected directly into the cell. Losses comprise of front glass losses and ARC losses which contributed to a total of 0.86% and 1.03% for homogenizers with straight and tapered sidewalls, respectively. For tapered homogenizers, when the base angle is  $40^\circ$ , the small angle fraction of reflected light increases leading to reduced side losses and increased top losses compared to a homogenizer with straight sidewalls. When the base angle is larger than  $80^\circ$ , no reflected rays were detected which means light can be totally redirected to the cell for both homogenizers.

**TABLE 1** Electrical parameters of a reference GaAs single-junction solar cell

Parameter	Value	Comment
$J_{sc}$ (A/cm <sup>2</sup> )	2.9	Unshaded short circuit current density under 100 Suns
$J_{01}$ (A/cm <sup>2</sup> )	$4.0 \times 10^{-20}$	Saturation current density associated with diffusion process
$J_{02, scr}$ (A/cm <sup>2</sup> )	$2.0 \times 10^{-11}$	Saturation current density in space charge regions
$J_{02, p}$ (A/cm <sup>2</sup> )	$1.0 \times 10^{-12}$	Saturation current density at the perimeter
$\rho_e$ ( $\Omega/\square$ )	110	Sheet resistance of emitter
$\rho_c$ ( $\Omega \text{ cm}^2$ )	$6.45 \times 10^{-6}$	Contact resistivity (of metal-semiconductor-contact)
$\rho_M$ ( $\Omega \text{ cm}$ )	$3.5 \times 10^{-6}$	Resistivity of metal fingers

The potential solar cell efficiency enhancement that could be achieved by using these shaped finger structures in a CPV system was estimated based on a reference GaAs single-junction solar cell reported by Steiner et al.<sup>22</sup> The electrical parameters of this reference cell are shown in Table 1. For this analysis, the short circuit current

Parameter	Homogenizer with straight sidewalls		Homogenizer with tapered sidewalls	
	RF	LDF with constant area	RF	LDF with constant area
Optical gain (%)	89.8	99.1	89.0	98.9
$J_{sc}$ (A/cm <sup>2</sup> )	2.6	2.9	2.6	2.9
$V_{oc}$ (V)	1.2	1.2	1.2	1.2
FF (%)	87.4	87.3	87.5	87.2
$\eta$ (%)	26.8	29.6	26.6	29.5

**TABLE 2** Cell performance of a CPV cell with RF and LDF structures estimated for homogenizers with straight and tapered sidewalls

density ( $J_{sc}$ ) was assumed to increase linearly with decreased shading losses, and the open circuit voltage ( $V_{oc}$ ) was calculated from the diode equation using the recombination current density ( $J_{01}$ ) listed in Table 1 and the estimated  $J_{sc}$ . The fill factor (FF) was then estimated by simulating an  $I$ - $V$  curve modeled using the two-diode equation to extract maximum power point. The potential solar cell efficiency enhancement was then computed using the obtained values for  $J_{sc}$ ,  $V_{oc}$ , and FF for the LDF structure as this was found in the analysis above to result in the highest optical efficiency of all the structures investigated. A finger grid comprising of LDF structures (base width 3.7  $\mu\text{m}$ ; base angle 85°) was compared to a similar grid of RF structures (width 5  $\mu\text{m}$ ; height 4  $\mu\text{m}$ ). The same finger spacing (50  $\mu\text{m}$ ) and finger cross-sectional area (20  $\mu\text{m}^2$ ) were used for both cases, thereby ensuring the same lateral emitter and finger resistance losses. The estimated efficiency results highly depend on the assumption made for the finger spacing and finger cross-sectional area. It was assumed that the cell series resistance was limited by the lateral emitter resistance or finger resistive loss, and consequently, any small differences in contact resistance arising from the different base area would have been negligible. The series resistance was calculated to be  $7.6 \times 10^{-3} \Omega \text{ cm}^2$ , which is comparable to the value calculated from Steiner et al.'s paper.<sup>22</sup> The  $J_{sc}$  for the base RF case was derated from the value reported in Table 1 to account for the finger shading (100% of the area of the RF structures across the cell surface) since the reported  $J_{sc}$  from Steiner et al.<sup>22</sup> was for an unshaded device.

Table 2 shows the electrical parameters estimated for CPV cells with the RF and LDF structures. With the increased optical gain, the value of  $J_{sc}$  for the LDF case increases by 10.3% and 11.2% relative compared to the base RF case for homogenizers with straight and tapered sidewalls, respectively. Since  $J_L$  only changes slightly and  $J_0$  does not change,  $V_{oc}$  would not change significantly. The base RF cell has a solar cell efficiency of 26.8% and 26.6% for straight homogenizers and tapered homogenizers, respectively. By changing to LDF structures, the solar cell efficiency can be increased to 29.6% and 29.5% for the investigated CPV systems with straight homogenizers and tapered homogenizers, respectively. This represents an absolute cell efficiency improvement of 2.8% and 3.0%, respectively.

Light diverting finger structures can redirect incoming light efficiently to the active area of the solar cell, therefore mitigating shading losses for CPV systems. However, their fabrication is challenging using typically used patterning and metal deposition methods such as photolithography and e-beam deposition. Precisely shaped, sharp edged structures are difficult to practically achieve. Saive et al.<sup>16</sup>

reported the use of gravure printing using conductive inks to produce triangular-shaped fingers on silicon solar cells. Although the described finger fabrication approach may be difficult to scale to the larger area industrial silicon cells, it could conceivably be applied to smaller, higher-value CPV cells and therefore demonstrates the feasibility of using shaped fingers to increase efficiency of CPV systems. Furthermore, even if the sharp edges of light diverting structures cannot be easily achieved, this study shows that TFs with a rounded cap, which can be achieved using metal plating processes, can still provide beneficial efficiency improvements.

## 4 | CONCLUSION

The optical efficiency and loss analysis for five light management finger designs for CPV systems with two refractive homogenizers was investigated in this study. Trapezoid finger structures were shown to result in higher optical efficiency than RFs with a maximum increase of 5.8% absolute due to the tilted surface increasing the redirected ray fraction and decreasing finger top surface reflection. Light scattering fingers with a V-groove cap and RCFs can both improve the optical efficiency by 2.7% for CPV systems with straight homogenizer sidewalls. However, VCF structures present no benefit in systems with tapered homogenizer sidewalls, while RCFs can slightly improve the performance with a maximum increase of 1.6%. Most reflected rays scatter outside the CPV system at the sidewalls or at the top surface, with the fraction depending on the finger structure. Light diverting fingers can improve the optical efficiency in CPV systems by up to 9.4% and 9.9% absolute, respectively, for homogenizers with straight and tapered sidewalls as the rays can be redirected to the cell directly. We show that application of LDF structures with constant finger number/spacing and finger cross-sectional area can increase the electrical cell efficiency by up to 3.0% absolute compared to a similar system with RFs. Efficiency improvements could be even greater when the entire module is optimized.

In conclusion, we have demonstrated how the profile of the front metal fingers can be used to effectively reduce the front metal shading loss in CPV systems resulting higher energy conversion efficiencies. Determination of the optimal shape of these fingers requires an optimization of light management in the entire CPV system, including the design of homogenizers which are routinely used to homogenize the flux across the receiving solar cell's surface. The additional processing does not add significant complexity since CPV cells

typically require high resolution patterning steps using higher cost processes such as photolithography. The addition of finger shaping processes would not therefore represent a large step change in processing complexity.

## ACKNOWLEDGMENTS

This program has been supported by the Australian Government through the Australian Renewable Energy Agency (ARENA) through Grant 2017/RND002 and Australian Research Council (ARC) through Future Fellowship (FT170100447; Alison Lennon) and DECRA (DE210100453; Udo Römer). Responsibility for the views, information, or advice expressed herein is not accepted by the Australian Government.

## ORCID

Mengdi Liu  <https://orcid.org/0000-0002-1812-7232>

Udo Römer  <https://orcid.org/0000-0002-9290-321X>

Nicholas J. Ekins-Daukes  <https://orcid.org/0000-0003-1875-9739>

Alison Lennon  <https://orcid.org/0000-0002-9166-7171>

## REFERENCES

- Swanson RM. The promise of concentrators. *Prog Photovolt Res Appl*. 2000;8(1):93-111. doi:10.1002/(SICI)1099-159X(200001/02)8:1<93::AID-PIP303>3.0.CO;2-S
- Hirst LC, Ekins-Daukes NJ. Fundamental losses in solar cells. *Prog Photovolt Res Appl*. 2011;19(3):286-293. doi:10.1002/PIP.1024
- Baudrit M, Algora C. Theoretical optimization of GaInP/GaAs dual-junction solar cell: toward a 36% efficiency at 1000 suns. *Phys Status Solidi Appl Mater Sci*. 2010;207(2):474-478. doi:10.1002/PSSA.200925210
- Algora C, Ortiz E, Rey-Stolle I, et al. A GaAs solar cell with an efficiency of 26.2% at 1000 suns and 25.0% at 2000 suns. *IEEE T Electron Dev*. 2001;48(5):840-844. doi:10.1109/16.918225
- Algora C, Díaz V. Influence of series resistance on guidelines for manufacture of concentrator p-on-n GaAs solar cells. *Prog Photovolt Res Appl*. 2000;8(2):211-225. doi:10.1002/(SICI)1099-159X(200003/04)8:2<211::AID-PIP291>3.0.CO;2-D
- Gupta DK, Barink M, Langelaar M. CPV solar cell modeling and metalization optimization. *Sol Energy*. 2018;159:868-881. doi:10.1016/j.solener.2017.11.015
- Bissels GMMW, Asselbergs MAH, Schermer JJ, Haverkamp EJ, Smeenk NJ, Vlieg E. A genuine circular contact grid pattern for solar cells. *Prog Photovolt Res Appl*. 2011;19(5):517-526. doi:10.1002/pip.1076
- Ward JS, Duda A, Friedman DJ, Geisz J, McMahan W, Young M. High aspect ratio electrodeposited Ni/Au contacts for GaAs-based III-V concentrator solar cells. *Prog Photovolt Res Appl*. 2015;23(5):646-653. doi:10.1002/pip.2490
- Verlinden P. Advanced module concepts. *Photovolt Sol Energy*. 2017; 502-510. doi:10.1002/9781118927496.ch45
- Mittag M, Beinert AJ, Rendler LC, Ebert M, Eitner U, "Triangular ribbons for improved module efficiency," 32nd EU PVSEC Conference and Intersolar Exhibition. 2019;169-172.
- Muehleisen W, Neumaier L, Hirschl C, et al. Comparison of output power for solar cells with standard and structured ribbons. *EPJ Photo-voltaics*. 2016;7:70701. doi:10.1051/epjpv/2016003
- O'Neill MB and Ma J, "Light redirecting film useful with solar modules," US Patent No. 10510913, 2019
- Haedrich I, Ernst M. Impact of angular irradiance distributions on coupling gains and energy yield of cell interconnection designs in silicon solar modules in tracking and fixed systems. *J Phys D Appl Phys*. 2021; 54(22):224003. doi:10.1088/1361-6463/abe967
- Li Y, Song N, Hsiao PC, Mungra M, Ouyang Z, Haedrich I, Ernst M, Newman B, Jansen M, Zhu C, Lv J, "Comparison of ribbon light management designs for photovoltaic modules," In 2019 IEEE 46th Photovoltaic Specialists Conference (PVSC). 2019;2219-2222 doi:10.1109/PVSC40753.2019.8980792
- Kik PG. Catoptric electrodes: transparent metal electrodes using shaped surfaces. *Opt Lett*. 2014;39(17):5114-5117. doi:10.1364/OL.39.005114
- Saive R, Borsuk AM, Emmer HS, et al. Effectively transparent front contacts for optoelectronic devices. *Adv Opt Mater*. 2016;4(10):1470-1474. doi:10.1002/adom.201600252
- Baig H, Heasman KC, Mallick TK. Non-uniform illumination in concentrating solar cells. *Renew Sust Energy Rev*. 2012;16(8):5890-5909. doi:10.1016/j.rser.2012.06.020
- Mitchell KW, "Computer analysis of resistance and non-uniform illumination effects on concentrator solar cells," in 1977 International Electron Devices Meeting, 2008, 229-232. doi:10.1109/iedm.1977.189214.
- Steiner M, Kiefel P, Siefert G, et al. CPV module design optimization for advanced multi-junction solar cell concepts. *AIP Conf Proc*. 2015; 1679(1):100005. doi:10.1063/1.4931552
- Helmers H, Thor WY, Schmidt T, van Rooyen DW, Bett AW. Optical analysis of deviations in a concentrating photovoltaics central receiver system with a flux homogenizer. *Appl Opt*. 2013;52(13): 2974-2984. doi:10.1364/AO.52.002974
- Osterwald CR, Siefert G. CPV multijunction solar cell characterization. In: *Handbook of Concentrator Photovoltaic Technology*. John Wiley & Sons, Ltd; 2016:589-614. doi:10.1002/9781118755655.ch10
- Steiner M, Philipps SP, Hermle M, Bett AW, Dimroth F. Validated front contact grid simulation for GaAs solar cells under concentrated sunlight. *Prog Photovolt Res Appl*. 2011;19(1):73-83. doi:10.1002/pip.989

**How to cite this article:** Liu M, Römer U, Ekins-Daukes NJ, Lennon A. Optical analysis of light management for finger designs in CPV systems. *Prog Photovolt Res Appl*. 2022;1-9. doi:10.1002/pip.3570